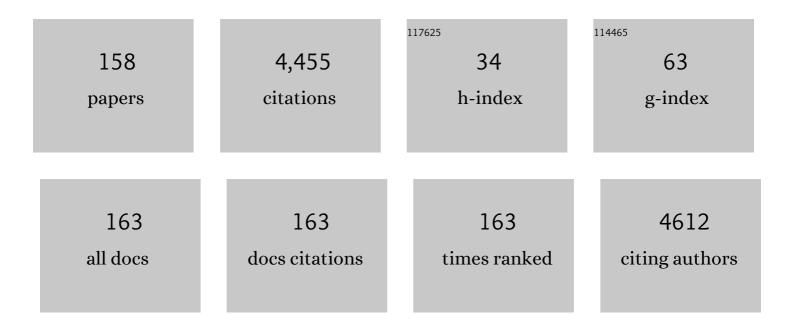
## **Einar Heiberg**

List of Publications by Year in descending order

Source: https://exaly.com/author-pdf/8544896/publications.pdf Version: 2024-02-01



FINIAD HEIREDC

#	Article	IF	CITATIONS
1	Design and validation of Segment - freely available software for cardiovascular image analysis. BMC Medical Imaging, 2010, 10, 1.	2.7	725
2	Transit of Blood Flow Through the Human Left Ventricle Mapped by Cardiovascular Magnetic Resonance. Journal of Cardiovascular Magnetic Resonance, 2007, 9, 741-747.	3.3	187
3	Myocardium at Risk After Acute Infarction in Humans on Cardiac Magnetic Resonance. JACC: Cardiovascular Imaging, 2009, 2, 569-576.	5.3	184
4	Automated Quantification of Myocardial Infarction from MR Images by Accounting for Partial Volume Effects: Animal, Phantom, and Human Study. Radiology, 2008, 246, 581-588.	7.3	174
5	The quantitative relationship between longitudinal and radial function in left, right, and total heart pumping in humans. American Journal of Physiology - Heart and Circulatory Physiology, 2007, 293, H636-H644.	3.2	158
6	Effect of intravenous TRO40303 as an adjunct to primary percutaneous coronary intervention for acute ST-elevation myocardial infarction: MITOCARE study results. European Heart Journal, 2015, 36, 112-119.	2.2	154
7	Quantification of left and right ventricular kinetic energy using four-dimensional intracardiac magnetic resonance imaging flow measurements. American Journal of Physiology - Heart and Circulatory Physiology, 2012, 302, H893-H900.	3.2	117
8	Vortex Ring Formation in the Left Ventricle of the Heart: Analysis by 4D Flow MRI and Lagrangian Coherent Structures. Annals of Biomedical Engineering, 2012, 40, 2652-2662.	2.5	114
9	Rapid Initial Reduction of Hyperenhanced Myocardium After Reperfused First Myocardial Infarction Suggests Recovery of the Peri-Infarction Zone. Circulation: Cardiovascular Imaging, 2009, 2, 47-55.	2.6	113
10	Rapid short-duration hypothermia with cold saline and endovascular cooling before reperfusion reduces microvascular obstruction and myocardial infarct size. BMC Cardiovascular Disorders, 2008, 8, 7.	1.7	103
11	Quantification and visualization of cardiovascular 4D velocity mapping accelerated with parallel imaging or k-t BLAST: head to head comparison and validation at 1.5 T and 3 T. Journal of Cardiovascular Magnetic Resonance, 2011, 13, 55.	3.3	91
12	Semi-automatic quantification of myocardial infarction from delayed contrast enhanced magnetic resonance imaging. Scandinavian Cardiovascular Journal, 2005, 39, 267-275.	1.2	86
13	Left ventricular fluid kinetic energy time curves in heart failure from cardiovascular magnetic resonance 4D flow data. Journal of Cardiovascular Magnetic Resonance, 2015, 17, 111.	3.3	76
14	Vortex ring behavior provides the epigenetic blueprint for the human heart. Scientific Reports, 2016, 6, 22021.	3.3	69
15	Assessment of myocardium at risk with contrast enhanced steady-state free precession cine cardiovascular magnetic resonance compared to single-photon emission computed tomography. Journal of Cardiovascular Magnetic Resonance, 2010, 12, 25.	3.3	67
16	A new automatic algorithm for quantification of myocardial infarction imaged by late gadolinium enhancement cardiovascular magnetic resonance: experimental validation and comparison to expert delineations in multi-center, multi-vendor patient data. Journal of Cardiovascular Magnetic Resonance, 2016, 18, 27.	3.3	67
17	Three-dimensional flow characterization using vector pattern matching. IEEE Transactions on Visualization and Computer Graphics, 2003, 9, 313-319.	4.4	61
18	Contribution of mitral annular excursion and shape dynamics to total left ventricular volume change. American Journal of Physiology - Heart and Circulatory Physiology, 2004, 287, H1836-H1841.	3.2	60

#	Article	IF	CITATIONS
19	Contrast-Enhanced CMR Overestimates Early Myocardial Infarct Size. JACC: Cardiovascular Imaging, 2015, 8, 1379-1389.	5.3	55
20	Quantification of left and right atrial kinetic energy using four-dimensional intracardiac magnetic resonance imaging flow measurements. Journal of Applied Physiology, 2013, 114, 1472-1481.	2.5	53
21	Time resolved three-dimensional automated segmentation of the left ventricle. , 2005, , .		52
22	Size and transmural extent of first-time reperfused myocardial infarction assessed by cardiac magnetic resonance can be estimated by 12-lead electrocardiogram. American Heart Journal, 2005, 150, 920.e1-920.e9.	2.7	49
23	Noninvasive Quantification of Pressure-Volume Loops From Brachial Pressure and Cardiovascular Magnetic Resonance. Circulation: Cardiovascular Imaging, 2019, 12, e008493.	2.6	49
24	Multi-vendor, multicentre comparison of contrast-enhanced SSFP and T2-STIR CMR for determining myocardium at risk in ST-elevation myocardial infarction. European Heart Journal Cardiovascular Imaging, 2016, 17, 744-753.	1.2	47
25	Rationale and Design of the †MITOCARE' Study: A Phase II, Multicenter, Randomized, Double-Blind, Placebo-Controlled Study to Assess the Safety and Efficacy of TRO40303 for the Reduction of Reperfusion Injury in Patients Undergoing Percutaneous Coronary Intervention for Acute Myocardial Infarction, Cardiology, 2012, 123, 201-207.	1.4	46
26	On estimating intraventricular hemodynamic forces from endocardial dynamics: A comparative study with 4D flow MRI. Journal of Biomechanics, 2017, 60, 203-210.	2.1	46
27	Self-gated fetal cardiac MRI with tiny golden angle iGRASP: A feasibility study. Journal of Magnetic Resonance Imaging, 2017, 46, 207-217.	3.4	45
28	Left and right ventricular hemodynamic forces in healthy volunteers and elite athletes assessed with 4D flow magnetic resonance imaging. American Journal of Physiology - Heart and Circulatory Physiology, 2017, 312, H314-H328.	3.2	45
29	Disturbed left and right ventricular kinetic energy in patients with repaired tetralogy of Fallot: pathophysiological insights using 4D-flow MRI. European Radiology, 2018, 28, 4066-4076.	4.5	45
30	ANDEAN SPECIATION AND VICARIANCE IN NEOTROPICAL MACROCARPAEA (GENTIANACEAE–HELIEAE) <sup>1</sup> . Annals of the Missouri Botanical Garden, 2009, 96, 450-469.	1.3	44
31	Whole-heart four-dimensional flow can be acquired with preserved quality without respiratory gating, facilitating clinical use: a head-to-head comparison. BMC Medical Imaging, 2015, 15, 20.	2.7	42
32	Validation and reproducibility of cardiovascular 4D-flow MRI from two vendors using 2 <b>×</b> 2 parallel imaging acceleration in pulsatile flow phantom and inÂvivo with and without respiratory gating. Acta Radiologica, 2019, 60, 327-337.	1.1	41
33	Sources of variability in quantification of cardiovascular magnetic resonance infarct size - reproducibility among three core laboratories. Journal of Cardiovascular Magnetic Resonance, 2017, 19, 62.	3.3	40
34	Cardiovascular Magnetic Resonance to Predict Appropriate Implantable Cardioverter Defibrillator Therapy in Ischemic and Nonischemic Cardiomyopathy Patients Using Late Gadolinium Enhancement Border Zone. Circulation: Cardiovascular Imaging, 2017, 10, .	2.6	39
35	The relationship between longitudinal, lateral, and septal contribution to stroke volume in patients with pulmonary regurgitation and healthy volunteers. American Journal of Physiology - Heart and Circulatory Physiology, 2014, 306, H895-H903.	3.2	38
36	Independent validation of fourâ€dimensional flow MR velocities and vortex ring volume using particle imaging velocimetry and planar laserâ€Induced fluorescence. Magnetic Resonance in Medicine, 2016, 75, 1064-1075.	3.0	35

#	Article	IF	CITATIONS
37	Time-resolved tracking of the atrioventricular plane displacement in Cardiovascular Magnetic Resonance (CMR) images. BMC Medical Imaging, 2017, 17, 19.	2.7	35
38	Kinematics of the heart: strain-rate imaging from time-resolved three-dimensional phase contrast MRI. IEEE Transactions on Medical Imaging, 2002, 21, 1105-1109.	8.9	33
39	Validation and Development of a New Automatic Algorithm for Time-Resolved Segmentation of the Left Ventricle in Magnetic Resonance Imaging. BioMed Research International, 2015, 2015, 1-12.	1.9	33
40	An Improved Method for Automatic Segmentation of the Left Ventricle in Myocardial Perfusion SPECT. Journal of Nuclear Medicine, 2009, 50, 205-213.	5.0	31
41	Sample Size in Clinical Cardioprotection Trials Using Myocardial Salvage Index, Infarct Size, or Biochemical Markers as Endpoint. Journal of the American Heart Association, 2016, 5, e002708.	3.7	31
42	Decreased Diastolic Ventricular Kinetic Energy in Young Patients with Fontan Circulation Demonstrated by Four-Dimensional Cardiac Magnetic Resonance Imaging. Pediatric Cardiology, 2017, 38, 669-680.	1.3	30
43	Variable velocity encoding in a threeâ€dimensional, threeâ€directional phase contrast sequence: Evaluation in phantom and volunteers. Journal of Magnetic Resonance Imaging, 2012, 36, 1450-1459.	3.4	28
44	Hemodynamic forces using four-dimensional flow MRI: an independent biomarker of cardiac function in heart failure with left ventricular dyssynchrony?. American Journal of Physiology - Heart and Circulatory Physiology, 2018, 315, H1627-H1639.	3.2	27
45	Pulmonary Blood Volume Variation Decreases after Myocardial Infarction in Pigs: A Quantitative and Noninvasive MR Imaging Measure of Heart Failure. Radiology, 2010, 256, 415-423.	7.3	26
46	Volume Tracking: A new method for quantitative assessment and visualization of intracardiac blood flow from three-dimensional, time-resolved, three-component magnetic resonance velocity mapping. BMC Medical Imaging, 2011, 11, 10.	2.7	25
47	Freeâ€breathing fetal cardiac MRI with doppler ultrasound gating, compressed sensing, and motion compensation. Journal of Magnetic Resonance Imaging, 2020, 51, 260-272.	3.4	25
48	Quantitative polar representation of left ventricular myocardial perfusion, function and viability using SPECT and cardiac magnetic resonance: initial results. Clinical Physiology and Functional Imaging, 2005, 25, 215-222.	1.2	24
49	Altered biventricular hemodynamic forces in patients with repaired tetralogy of Fallot and right ventricular volume overload because of pulmonary regurgitation. American Journal of Physiology - Heart and Circulatory Physiology, 2018, 315, H1691-H1702.	3.2	24
50	Hemodynamic forces in the left and right ventricles of the human heart using 4D flow magnetic resonance imaging: Phantom validation, reproducibility, sensitivity to respiratory gating and free analysis software. PLoS ONE, 2018, 13, e0195597.	2.5	24
51	The endocardial extent of reperfused first-time myocardial infarction is more predictive of pathologic Q waves than is infarct transmurality: a magnetic resonance imaging study. Clinical Physiology and Functional Imaging, 2007, 27, 101-108.	1.2	23
52	Spatial evolutionary and ecological vicariance analysis (SEEVA), a novel approach to biogeography and speciation research, with an example from Brazilian Gentianaceae. Journal of Biogeography, 2011, 38, 1841-1854.	3.0	23
53	Semi-automatic segmentation of myocardium at risk in T2-weighted cardiovascular magnetic resonance. Journal of Cardiovascular Magnetic Resonance, 2012, 14, 20.	3.3	22
54	Importance of standardizing timing of hematocrit measurement when using cardiovascular magnetic resonance to calculate myocardial extracellular volume (ECV) based on pre- and post-contrast T1 mapping. Journal of Cardiovascular Magnetic Resonance, 2018, 20, 46.	3.3	22

#	Article	IF	CITATIONS
55	Regional Stress-Induced Ischemia in Non-fibrotic Hypertrophied Myocardium in Young HCM Patients. Pediatric Cardiology, 2015, 36, 1662-1669.	1.3	20
56	Regional contribution to ventricular stroke volume is affected on the left side, but not on the right in patients with pulmonary hypertension. International Journal of Cardiovascular Imaging, 2016, 32, 1243-1253.	1.5	20
57	Extent of Myocardium at Risk for Left Anterior Descending Artery, Right Coronary Artery, and Left Circumflex Artery Occlusion Depicted by Contrast-Enhanced Steady State Free Precession and T2-Weighted Short Tau Inversion Recovery Magnetic Resonance Imaging. Circulation: Cardiovascular Imaging, 2016, 9.	2.6	20
58	Vectorcardiogram synthesized from the 12-lead electrocardiogram to image ischemia. Journal of Electrocardiology, 2009, 42, 190-197.	0.9	19
59	Parallel simulations for QUAntifying RElaxation magnetic resonance constants (SQUAREMR): an example towards accurate MOLLI T1 measurements. Journal of Cardiovascular Magnetic Resonance, 2015, 17, 104.	3.3	19
60	Assessment of diastolic function and atrial remodeling byÂMRI - validation and correlation with echocardiography and filling pressure. Physiological Reports, 2018, 6, e13828.	1.7	18
61	Infarct quantification using 3D inversion recovery and 2D phase sensitive inversion recovery; validation in patients and ex vivo. BMC Cardiovascular Disorders, 2013, 13, 110.	1.7	16
62	Accuracy of four-dimensional phase-contrast velocity mapping for blood flow visualizations: a phantom study. Acta Radiologica, 2013, 54, 663-671.	1.1	16
63	Development of an automated method for display of ischemic myocardium from simulated electrocardiograms. Journal of Electrocardiology, 2009, 42, 204-212.	0.9	15
64	Development and validation of a new automatic algorithm for quantification of left ventricular volumes and function in gated myocardial perfusion SPECT using cardiac magnetic resonance as reference standard. Journal of Nuclear Cardiology, 2011, 18, 874-885.	2.1	15
65	Validation and development of a new automatic algorithm for time resolved segmentation of the left ventricle in magnetic resonance imaging. Journal of Cardiovascular Magnetic Resonance, 2015, 17, P68.	3.3	15
66	Required temporal resolution for accurate thoracic aortic pulse wave velocity measurements by phase-contrast magnetic resonance imaging and comparison with clinical standard applanation tonometry. BMC Cardiovascular Disorders, 2016, 16, 110.	1.7	15
67	Vortexâ€ring mixing as a measure of diastolic function of the human heart: Phantom validation and initial observations in healthy volunteers and patients with heart failure. Journal of Magnetic Resonance Imaging, 2016, 43, 1386-1397.	3.4	15
68	A new vessel segmentation algorithm for robust blood flow quantification from twoâ€dimensional phaseâ€contrast magnetic resonance images. Clinical Physiology and Functional Imaging, 2019, 39, 327-338.	1.2	15
69	Longitudinal strain from velocity encoded cardiovascular magnetic resonance: a validation study. Journal of Cardiovascular Magnetic Resonance, 2013, 15, 15.	3.3	14
70	Echocardiographic global longitudinal strain is associated with infarct size assessed by cardiac magnetic resonance in acute myocardial infarction. Echo Research and Practice, 2019, 6, 81-89.	2.5	14
71	Persistent decline in longitudinal and radial strain after coronary microembolization detected on velocity encoded phase contrast magnetic resonance imaging. Journal of Magnetic Resonance Imaging, 2009, 30, 69-76.	3.4	12
72	Validation of T1 and T2 algorithms for quantitative MRI: performance by a vendor-independent software. BMC Medical Imaging, 2016, 16, 46.	2.7	12

#	Article	IF	CITATIONS
73	Feasibility of Patient Specific Aortic Blood Flow CFD Simulation. Lecture Notes in Computer Science, 2006, 9, 257-263.	1.3	11
74	Automatic segmentation of myocardium at risk from contrast enhanced SSFP CMR: validation against expert readers and SPECT. BMC Medical Imaging, 2016, 16, 19.	2.7	11
75	Independent validation of metric optimized gating for fetal cardiovascular phaseâ€contrast flow imaging. Magnetic Resonance in Medicine, 2019, 81, 495-503.	3.0	11
76	Automated left atrial time-resolved segmentation in MRI long-axis cine images using active contours. BMC Medical Imaging, 2021, 21, 101.	2.7	10
77	Superâ€Resolution Cine Image Enhancement for Fetal Cardiac Magnetic Resonance Imaging. Journal of Magnetic Resonance Imaging, 2022, 56, 223-231.	3.4	10
78	An automatic method for quantification of myocardium at risk from myocardial perfusion SPECT in patients with acute coronary occlusion. Journal of Nuclear Cardiology, 2010, 17, 831-840.	2.1	9
79	Regional wall function before and after acute myocardial infarction; an experimental study in pigs. BMC Cardiovascular Disorders, 2014, 14, 118.	1.7	9
80	Validation of a new t2* algorithm and its uncertainty value for cardiac and liver iron load determination from MRI magnitude images. Magnetic Resonance in Medicine, 2016, 75, 1717-1729.	3.0	9
81	Longitudinal left ventricular function is globally depressed within a week of <scp>STEMI</scp> . Clinical Physiology and Functional Imaging, 2018, 38, 1029-1037.	1.2	9
82	Quantification of myocardium at risk in myocardial perfusion SPECT by coâ€registration and fusion with delayed contrastâ€enhanced magnetic resonance imaging – an experimental <i>ex vivo</i> study. Clinical Physiology and Functional Imaging, 2012, 32, 33-38.	1.2	8
83	Automatic lung segmentation in functional SPECT images using active shape models trained on reference lung shapes from CT. Annals of Nuclear Medicine, 2018, 32, 94-104.	2.2	8
84	Nonâ€invasive quantification of pressureâ€volume loops from cardiovascular magnetic resonance at rest and during dobutamine stress. Clinical Physiology and Functional Imaging, 2021, 41, 467-470.	1.2	8
85	Computer-assisted calculation of myocardial infarct size shortens the evaluation time of contrast-enhanced cardiac MRI. Clinical Physiology and Functional Imaging, 2007, 28, 071116231949002-???.	1.2	7
86	Simulation of aortopulmonary collateral flow in Fontan patients for use in prediction of interventional outcomes. Clinical Physiology and Functional Imaging, 2018, 38, 622-629.	1.2	7
87	Alterations in ventricular pumping in patients with atrial septal defect at rest, during dobutamine stress and after defect closure. Clinical Physiology and Functional Imaging, 2018, 38, 830-839.	1.2	7
88	The significance of STâ€elevation in aVL in anterolateral myocardial infarction: An assessment by cardiac magnetic resonance imaging. Annals of Noninvasive Electrocardiology, 2018, 23, e12580.	1.1	7
89	Functional Contribution ofÂCircumferential Versus Longitudinal Strain. Journal of the American College of Cardiology, 2018, 71, 254-255.	2.8	6
90	Cardiac Magnetic Resonance Evaluation of the Extent of Myocardial Injury in Patients with Inferior ST Elevation Myocardial Infarction and Concomitant ST Depression in Leads V1–V3: Analysis from the MITOCARE Study. Cardiology, 2018, 140, 178-185.	1.4	6

#	Article	IF	CITATIONS
91	MVnet: automated time-resolved tracking of the mitral valve plane in CMR long-axis cine images with residual neural networks: a multi-center, multi-vendor study. Journal of Cardiovascular Magnetic Resonance, 2021, 23, 137.	3.3	6
92	Volumetric velocity measurements in restricted geometries using spiral sampling: a phantom study. Magnetic Resonance Materials in Physics, Biology, and Medicine, 2015, 28, 103-118.	2.0	5
93	Myocardium at risk assessed by electrocardiographic scores and cardiovascular magnetic resonance - a MITOCARE substudy. Journal of Electrocardiology, 2017, 50, 725-731.	0.9	5
94	Gender but not diabetes, hypertension or smoking affects infarct evolution in ST-elevation myocardial infarction patients – data from the CHILL-MI, MITOCARE and SOCCER trials. BMC Cardiovascular Disorders, 2019, 19, 161.	1.7	5
95	Valvular imaging in the era of featureâ€ŧracking: A sliceâ€following cardiac MR sequence to measure mitral flow. Journal of Magnetic Resonance Imaging, 2020, 51, 1412-1421.	3.4	5
96	Atrioventricular plane displacement versus mitral and tricuspid annular plane systolic excursion: A comparison between cardiac magnetic resonance and Mâ€node echocardiography. Clinical Physiology and Functional Imaging, 2021, 41, 262-270.	1.2	5
97	FourFlow - open source code software for quantification and visualization of time-resolved three-directional phase contrast magnetic resonance velocity mapping. Journal of Cardiovascular Magnetic Resonance, 2012, 14, .	3.3	4
98	Quantification of left and right atrial kinetic energy using four-dimensional intracardiac magnetic resonance imaging flow measurements. Journal of Cardiovascular Magnetic Resonance, 2013, 15, P218.	3.3	4
99	Validation of an automated method to quantify stress-induced ischemia and infarction in rest-stress myocardial perfusion SPECT. Journal of Nuclear Cardiology, 2014, 21, 503-518.	2.1	4
100	Quantification of myocardial salvage by myocardial perfusion SPECT and cardiac magnetic resonance — reference standards for ECG development. Journal of Electrocardiology, 2014, 47, 525-534.	0.9	4
101	Correlation of anteroseptal ST elevation with myocardial infarction territories through cardiovascular magnetic resonance imaging. Journal of Electrocardiology, 2018, 51, 563-568.	0.9	4
102	Quantification of left ventricular contribution to stroke work by longitudinal and radial force-length loops. Journal of Applied Physiology, 2020, 129, 880-890.	2,5	4
103	TVnet: Automated Time-Resolved Tracking of the Tricuspid Valve Plane inÂMRI Long-Axis Cine Images with aÂDual-Stage Deep Learning Pipeline. Lecture Notes in Computer Science, 2021, , 567-576.	1.3	4
104	Diastolic vortex ring formation in the human left ventricle: quantitative analysis using Lagrangian coherent structures and 4D cardiovascular magnetic resonance velocity mapping. Journal of Cardiovascular Magnetic Resonance, 2012, 14, .	3.3	3
105	Evolution of left ventricular function among subjects with ST-elevation myocardial infarction after percutaneous coronary intervention. BMC Cardiovascular Disorders, 2020, 20, 309.	1.7	3
106	Anterior STEMI associated with decreased strain in remote cardiac myocardium. International Journal of Cardiovascular Imaging, 2021, , 1.	1.5	3
107	Pulse Wave Velocity Measurements by Magnetic Resonance Imaging in Neonates and Adolescents: Methodological Aspects and Their Clinical Implications. Pediatric Cardiology, 2022, , 1.	1.3	3
108	Ventricular longitudinal function by cardiovascular magnetic resonance predicts cardiovascular morbidity in HFrEF patients. ESC Heart Failure, 2022, 9, 2313-2324.	3.1	3

#	Article	IF	CITATIONS
109	Haemodynamic leftâ€ventricular changes during dobutamine stress in patients with atrial septal defect assessed with magnetic resonance imagingâ€based pressure–volume loops. Clinical Physiology and Functional Imaging, 2022, 42, 422-429.	1.2	3
110	Normal values for wall thickening by magnetic resonance imaging. Journal of Cardiovascular Magnetic Resonance, 2009, 11, .	3.3	2
111	Validation of blood flow partitioning in 4D phase contrast CMR measurements using lagrangian coherent structures. Journal of Cardiovascular Magnetic Resonance, 2011, 13, .	3.3	2
112	A new validated T2* analysis method with certainty estimates for cardiac and liver iron load determination. Journal of Cardiovascular Magnetic Resonance, 2015, 17, P52.	3.3	2
113	Whole-heart 4D flow can be acquired with preserved quality without respiratory gating facilitating clinical use. Journal of Cardiovascular Magnetic Resonance, 2015, 17, .	3.3	2
114	Cloud GPU-based simulations for SQUAREMR. Journal of Magnetic Resonance, 2017, 274, 80-88.	2.1	2
115	Correlation of ST changes in leads V4–V6 to area of ischemia by CMR in inferior STEMI. Scandinavian Cardiovascular Journal, 2018, 52, 189-195.	1.2	2
116	Appropriateness of anteroseptal myocardial infarction nomenclature evaluated by late gadolinium enhancement cardiovascular magnetic resonance imaging. Journal of Electrocardiology, 2018, 51, 218-223.	0.9	2
117	Stationary tissue background correction increases the precision of clinical evaluation of intra-cardiac shunts by cardiovascular magnetic resonance. Scientific Reports, 2020, 10, 5053.	3.3	2
118	Automated calculation of infarct transmurality. , 2007, , .		1
119	Myocardium at risk and myocardial salvage after acute infarction in humans; quantification by magnetic resonance imaging. Journal of Cardiovascular Magnetic Resonance, 2009, 11, .	3.3	1
120	Evolution of left ventricular strain after a first time myocardial infarction. A study using velocity encoded magnetic resonance imaging. Journal of Cardiovascular Magnetic Resonance, 2009, 11, .	3.3	1
121	Improved quantification of T2* relaxation in magnetic resonance imaging. Journal of Cardiovascular Magnetic Resonance, 2011, 13, .	3.3	1
122	Performance of contrast enhanced SSFP and T2-weighted imaging for determining myocardium at risk in a multi-vendor, multi-center setting- data from the MITOCARE and CHILL-MI trials. Journal of Cardiovascular Magnetic Resonance, 2015, 17, P194.	3.3	1
123	Regional contributions to ventricular stroke volumes are affected on the left side, and not on the right in patients with pulmonary hypertension. Journal of Cardiovascular Magnetic Resonance, 2015, 17, P294.	3.3	1
124	Phantom validation of 4D flow: independent validation of vortex ring volume quantification using planar laser-induced fluorescence. Journal of Cardiovascular Magnetic Resonance, 2015, 17, P38.	3.3	1
125	A novel tool for phase contrast MR-derived pulse wave velocity measurement - validation against applanation tonometry and phantom studies. Journal of Cardiovascular Magnetic Resonance, 2015, 17, P40.	3.3	1
126	Design of clinical cardioprotection trials using CMR: impact of myocardial salvage index and a narrow inclusion window on sample size. Journal of Cardiovascular Magnetic Resonance, 2015, 17, P90.	3.3	1

#	Article	IF	CITATIONS
127	Validation and quantification of left ventricular function during exercise and free breathing from real-time cardiac magnetic resonance images. Scientific Reports, 2022, 12, 5611.	3.3	1
128	Non-invasive quantification of pressure–volume loops in patients with Fontan circulation. BMC Cardiovascular Disorders, 2022, 22, .	1.7	1
129	1017 Computer-assisted calculation of myocardial infarct size shortens the evaluation time of contrast enhanced cardiac MRI. Journal of Cardiovascular Magnetic Resonance, 2008, 10, .	3.3	Ο
130	1028 The hyperenhanced region assessed by ex vivo DE-MRI is consistently larger than infarct size determined by TTC staining in the acute phase of reperfused ischemic myocardial injury. Journal of Cardiovascular Magnetic Resonance, 2008, 10, .	3.3	0
131	1080 Strain analysis using magnetic resonance imaging can independently identify affected vessel after acute coronary syndrome. Journal of Cardiovascular Magnetic Resonance, 2008, 10, .	3.3	0
132	1106 Normal values for strain calculated from velocity encoded MRI. Journal of Cardiovascular Magnetic Resonance, 2008, 10, A231.	3.3	0
133	1107 Quantification of left ventricular strain using turbo field echo produces less variable data than using fast field echo. Journal of Cardiovascular Magnetic Resonance, 2008, 10, .	3.3	0
134	Volume tracking – a novel method for visualization and quantification of intracardiac blood flow from 3D time resolved phase contrast MRI. Journal of Cardiovascular Magnetic Resonance, 2009, 11, .	3.3	0
135	A novel prototype-based segmentation requiring only five training cases applied to MR angiography. Journal of Cardiovascular Magnetic Resonance, 2009, 11, .	3.3	Ο
136	Quantification of left ventricular kinetic energy using 4D flow MRI. Journal of Cardiovascular Magnetic Resonance, 2010, 12, .	3.3	0
137	Myocardium at risk with contrast enhanced SSFP compared to myocardial perfusion SPECT. Journal of Cardiovascular Magnetic Resonance, 2010, 12, .	3.3	0
138	Global and regional function quantified on MRI before and after surgical ventricular reconstruction. Journal of Cardiovascular Magnetic Resonance, 2010, 12, .	3.3	0
139	Regional myocardial strain at rest as assessed by velocity-encoded CMR remain unchanged in endurance trained athletes compared to normal subjects. Journal of Cardiovascular Magnetic Resonance, 2010, 12, .	3.3	0
140	Intracardiac cardiovascular magnetic resonance velocity mapping: comparison of k-t BLAST and SENSE accelerated 4D acquisitions with 2D-flow at 1.5 T and 3 T. Journal of Cardiovascular Magnetic Resonance, 2010, 12, .	3.3	0
141	Automatic segmentation of myocardium at risk in T2-weighted cardiovascular magnetic resonance. Journal of Cardiovascular Magnetic Resonance, 2012, 14, .	3.3	Ο
142	Quantification of the contribution of septal movement to stroke volume in healthy subjects, athletes, patients with pulmonary insufficiency and patients with pulmonary hypertension. Journal of Cardiovascular Magnetic Resonance, 2012, 14, .	3.3	0
143	Vortex formation ratio in heart failure compared to healthy volunteers at rest and during exercise. Journal of Cardiovascular Magnetic Resonance, 2013, 15, 065.	3.3	0
144	Comparison of methods for DE-CMR infarct size quantification - reproducibility among three core labs. Journal of Cardiovascular Magnetic Resonance, 2013, 15, P180.	3.3	0

#	Article	IF	CITATIONS
145	Semi-automatic segmentation of myocardium at risk from contrast enhanced SSFP images - validation against manual delineation and SPECT. Journal of Cardiovascular Magnetic Resonance, 2015, 17, Q127.	3.3	0
146	Phantom validation of 4D flow: independent validation of flow velocity quantification using particle imaging velocimetry. Journal of Cardiovascular Magnetic Resonance, 2015, 17, O18.	3.3	0
147	The extent of myocardium at risk for LAD, RCA and LCx using contrast enhanced SSFP and T2-weighted imaging. Journal of Cardiovascular Magnetic Resonance, 2015, 17, P139.	3.3	0
148	Prediction of appropriate ICD-therapy using infarct heterogeneity from CMR in patients with coronary artery disease. Journal of Cardiovascular Magnetic Resonance, 2015, 17, P165.	3.3	0
149	Sources of variability in quantification of CMR infarct size and their impact on sample size calculations - reproducibility among three core laboratories. Journal of Cardiovascular Magnetic Resonance, 2015, 17, .	3.3	0
150	Regional adenosine-induced hypoperfusion without hyperenhancement on LGE-MRI in young HCM patients: comparison to subjects at risk of HCM and healthy volunteers. Journal of Cardiovascular Magnetic Resonance, 2015, 17, Q51.	3.3	0
151	Alterations in right ventricular pumping in patients with atrial septal defect at rest and during dobutamine stress. Journal of Cardiovascular Magnetic Resonance, 2015, 17, Q86.	3.3	0
152	MR photography of 3D-MR images. Journal of Cardiovascular Magnetic Resonance, 2016, 18, P33.	3.3	0
153	New automatic algorithm for segmentation of myocardial scar in both inversion recovery and phase sensitive inversion recovery late gadolinium enhancement: validation against TTC and in multi-center, multi-vendor patient data. Journal of Cardiovascular Magnetic Resonance, 2016, 18, P221.	3.3	0
154	The Authors Reply:. JACC: Cardiovascular Imaging, 2016, 9, 1016-1017.	5.3	0
155	Response by Jablonowski et al to Letter Regarding Article, "Cardiovascular Magnetic Resonance to Predict Appropriate Implantable Cardioverter Defibrillator Therapy in Ischemic and Nonischemic Cardiomyopathy Patients Using Late Gadolinium Enhancement Border Zone: Comparison of Four Analysis Methods― Circulation: Cardiovascular Imaging, 2018, 11, e007333.	2.6	0
156	Current and Emerging Technologies for Cardiovascular Imaging. Series in Bioengineering, 2019, , 13-59.	0.6	0
157	Regional contributions to left ventricular stroke volume determined by cardiac magnetic resonance imaging in cardiac resynchronization therapy. BMC Cardiovascular Disorders, 2021, 21, 519.	1.7	0
158	Automated Measurements of Mitral and Tricuspid Annular Dimensions in Cardiovascular Magnetic Resonance. , 2022, , .		0